OXFORD

*Carcinogenesis*, 2016, Vol. 37, No. 11, 1052–1061

**doi:10.1093/carcin/bgw096**
Advance Access publication September 8, 2016
Original Manuscript

ORIGINAL MANUSCRIPT

# Honokiol suppresses pancreatic tumor growth, metastasis and desmoplasia by interfering with tumor–stromal cross-talk

Courey Averett[1], Arun Bhardwaj[1], Sumit Arora[1], Sanjeev K.Srivastava[1], Mohammad Aslam Khan[1], Aamir Ahmad[1], Seema Singh[1,2], James E.Carter[3], Moh'd Khushman[4] and Ajay P.Singh[1,2,*]

[1]Department of Oncologic Sciences, Mitchell Cancer Institute, [2]Department of Biochemistry and Molecular Biology, College of Medicine, [3]Department of Pathology, College of Medicine and [4]Department of Interdisciplinary Clinical Oncology, Mitchell Cancer Institute, University of South Alabama, 1660 Springhill Avenue, Mobile, AL 36604-1405, USA

*To whom correspondence should be addressed. Tel: +1 251 445 9843; Fax: +1 251 460 6994; Email: asingh@health.southalabama.edu

## Abstract

The poor clinical outcome of pancreatic cancer (PC) is largely attributed to its aggressive nature and refractoriness to currently available therapeutic modalities. We previously reported antitumor efficacy of honokiol (HNK), a phytochemical isolated from various parts of Magnolia plant, against PC cells in short-term *in vitro* growth assays. Here, we report that HNK reduces plating efficiency and anchorage-independent growth of PC cells and suppresses their migration and invasiveness. Furthermore, significant inhibition of pancreatic tumor growth by HNK is observed in orthotopic mouse model along with complete-blockage of distant metastases. Histological examination suggests reduced desmoplasia in tumors from HNK-treated mice, later confirmed by immunohistochemical analyses of myofibroblast and extracellular matrix marker proteins (α-SMA and collagen I, respectively). At the molecular level, HNK treatment leads to decreased expression of sonic hedgehog (SHH) and CXCR4, two established mediators of bidirectional tumor–stromal cross-talk, both *in vitro* and *in vivo*. We also show that the conditioned media (CM) from HNK-treated PC cells have little growth-inducing effect on pancreatic stellate cells (PSCs) that could be regained by the addition of exogenous recombinant SHH. Moreover, pretreatment of CM of vehicle-treated PC cells with SHH-neutralizing antibody abolishes their growth-inducing potential on PSCs. Likewise, HNK-treated PC cells respond poorly to CM from PSCs due to decreased CXCR4 expression. Lastly, we show that the transfection of PC cells with constitutively active IKKβ mutant reverses the suppressive effect of HNK on nuclear factor-kappaB activation and partially restores CXCR4 and SHH expression. Taken together, these findings suggest that HNK interferes with tumor–stromal cross-talk via downregulation of CXCR4 and SHH and decreases pancreatic tumor growth and metastasis.

## Introduction

Pancreatic cancer (PC) remains a clinical challenge despite significant advancements in our understanding of its molecular pathobiology (1). This year, it is predicted to inflict ~53 070 people and claim 41 780 lives to become the third leading cause of cancer-related deaths in the USA (2). Over the years, new treatment options have been tested either as single agents or as combination therapies; however, none has provided significantly superior benefit in patients' survival (3,4). Moreover, some therapies cause extreme side effects and thus not recommended to older patients (5). As a result, 5-year postdiagnosis survival rate of PC patients has remained between 4.0 and 7.0% for the past three decades (2). Clearly, there remains a dire need

**Received:** May 27, 2016; **Revised:** July 25, 2016; **Accepted:** September 2, 2016

**Abbreviations**

| | |
|---|---|
| CM | conditioned media |
| H&E | hematoxylin and eosin |
| HNK | honokiol |
| IHC | immunohistochemical |
| NF-κB | nuclear factor-kappaB |
| PC | pancreatic cancer |
| PSCs | pancreatic stellate cells |
| SHH | sonic hedgehog |
| α-SMA | alpha-smooth muscle actin |

for novel agents that are more effective, yet relatively safer, in curbing the aggressive growth of PC.

Natural compounds have made a significant impact on the anticancer drug discovery process (6). One-third of all the drugs approved by the United States Food and Drug Administration (USFDA) for cancer treatment are either natural compounds or their derivatives (7,8). Honokiol (HNK), a small biphenolic lignan consisting of a bioactive para-allyl and ortho-allyl phenols, is derived from various parts of the plants of *Magnolia* species (9). Lately, it has attracted a great deal of attention in cancer research due to its antitumor efficacy along with a desirable spectrum of bioavailability after intravenous administration in animal models (9–11). We also reported previously that it suppressed growth of PC cells by inducing $G_1$/S cell-cycle arrest and apoptosis (12). However, a more comprehensive examination of its anticancer efficacy remained to be explored.

In the present study, we evaluated the efficacy of HNK against long-term growth and malignant phenotypes of PC cells *in vitro* and in an orthotopic mouse model of PC, and delineated underlying molecular mechanisms. HNK reduced the plating efficiency, anchorage-independent growth, and migratory and invasive potential of PC cells. In addition, HNK treatment significantly inhibited the growth of orthotopic pancreatic tumors in nude mice. Moreover, no visible metastases were detected in any of the HNK-treated mice on bioluminescence and histological examinations. In addition, pancreatic tumors from HNK-treated group exhibited decreased desmoplasia as confirmed by immunostaining of extracellular matrix and myofibroblast marker proteins. Expression of CXCR4 and sonic hedgehog (SHH), two known promoters of tumor growth, metastasis and desmoplasia (13–17), was reduced in HNK-treated pancreatic tumor xenografts and in cancer cell lines *in vitro*. Further biochemical studies suggested the role of nuclear factor-kappaB (NF-κB) in suppression of CXCR4 and SHH expression. Together, these findings lend additional experimental and strong preclinical support for the candidacy of HNK as a novel and effective agent for PC therapy and prevention, either alone or in combination with other treatment modalities.

## Materials and methods

### Reagents, plasmids and antibodies

The following reagents were used in this study: Roswell Park Memorial Institute medium (RPMI-1640); Dulbecco's modified Eagle medium; penicillin and streptomycin (Invitrogen, Carlsbad, CA); fetal bovine serum (Atlanta Biologicals, Lawrenceville, GA); HNK (Cayman Chemical Company, Ann Arbor, MI); AMD3100 and Cremophor EL (Sigma–Aldrich, St Louis, MO); recombinant human SHH (R & D Systems, Minneapolis, MN); pGL4.32 (luc2P/NF-B-RE/Hygro) and pRL-TK plasmids (Promega, Madison, WI). pCMV-IKKβ S177E S181E (plasmid number 11105) (A. Rao Laboratory; procured through Addgene, Cambridge, MA); pCMV (Origene, Rockville, MD); X-tremeGENE HP DNA Transfection Reagent (Roche, Indianapolis, IN); western blotting SuperSignal West Femto Maximum sensitivity substrate kit (Thermo Scientific, Logan, UT); immunohistochemical (IHC) analysis reagent EZ-Dewax (Biogenex, Fremont, CA); background sniper, polymer and probe (Biocare Medical, Concord, CA); VivoGlo™ Luciferin (Promega, Madison, WI). The following antibodies were used: CXCR4 (1:1000; rabbit monoclonal), SHH, alpha-smooth muscle actin (α-SMA) (1:100, rabbit monoclonal) (Epitomics, Burlingame, CA), collagen I (1:100, rabbit polyclonal) (Abcam, Cambridge, MA), SHH-neutralizing antibody 5E1 [Developmental Studies Hybridoma Bank (DSHB), University of Iowa, Iowa City, IA (deposited by T.M.Jessell/S. Brenner-Morton)], mouse biotinylated anti-β-actin (1:20 000; Sigma–Aldrich) and horseradish peroxidase labeled secondary antibodies (1:2000; Santa Cruz Biotechnology, Dallas, TX).

### Cell culture and treatment

PC cells, MiaPaCa and Colo-357, were procured and maintained in culture as adherent monolayer as described earlier (18). Cell lines used in this study were authenticated by short tandem repeats genotyping (Genetica DNA Laboratories, Burlington, NC). For HNK treatment, stock solution (10 mM) of HNK was prepared in dimethyl sulfoxide, stored at −20°C and diluted at desired concentration with fresh complete medium immediately before use. An equal volume of dimethyl sulfoxide (<0.1%) was added to the control.

### Plating efficiency assay

Cells ($1\times10^3$ cells/well) were seeded in six-well plates and allowed to adhere and establish for 24 h. Subsequently, cells were treated with vehicle or various doses of HNK (0–5 μM). Fresh media containing HNK or vehicle was replaced after every third day. After 2 weeks, colonies were fixed with methanol, stained with crystal violet, photographed and counted using image analysis software (Gene Tools, Syngene, Frederick, MD).

### Soft-agar assay

Soft-agar assay was performed as described previously by us (19). Briefly, equal volumes of agarose (1.6%) and regular growth medium were mixed and plated to form bottom layer (0.8% agar growth medium) in six-well plates. Cells ($2.5\times10^3$ cells/ml) were suspended in regular culture media, mixed with equal volume of 0.6% agarose, and cell suspension-agar mix (2 ml) was seeded as top layer in each well and replenished with treatment media (vehicle or HNK), and incubated for 3 weeks. Fresh media containing HNK or vehicle was replaced every third day. Colonies were stained with 0.005% crystal violet in phosphate-buffered saline, observed using Nikon Eclipse microscope (Nikon Instruments) and counted in 10 randomly selected fields (×100 magnification).

### Migration and invasion assays

PC cells were grown in six-well plates to subconfluence level, treated with vehicle or varying concentrations of HNK (0–5 μM) for 48 h. Post-treatment, cells were trypsinized, counted and plated at equal density in the upper chamber of non-coated polyethylene teraphthalate membrane (Boyden Chamber, six-well insert, 8.0 μm; BD Biosciences) (for migration) or Matrigel-coated polycarbonate membrane (24-well insert, 8.0 μm, BD Biosciences) (for invasion) in serum-free medium. Media supplemented with 10% fetal bovine serum was used as chemoattractant in the lower chamber. Cells were allowed to migrate/invade for 16 h, and then cells remaining in the upper portion were removed. Cells that had migrated/invaded were fixed, stained with Diff-Quick cell staining kit (Dade Behring, Newark, DE), mounted on slides and counted in 10 random fields under microscope.

### Orthotopic xenograft study

All animal experiments were performed in compliance with Institutional Animal Care and Use Committee (IACUC) guidelines. Immunocompromised female mice (4–6 weeks old; Harlan Laboratories, Prattville, AL) were anesthetized with intraperitoneal (i.p.) injection of ketamine (100 mg/kg) and xylazine (15 mg/kg). Luciferase-tagged MiaPaCa cells ($1\times10^6$/50 μl) were injected into the pancreas of immunocompromised mice as described previously (19). Once tumor became palpable (~7 days after injection), the animals were randomly divided into two groups (six mice per group). One group received i.p. injection of HNK (150 mg/kg body weight, once

daily), whereas the other group received vehicle (Cremophor EL) only. Tumor growth was monitored weekly by bioluminescence imaging using Xenogen-IVIS-cooled CCD optical system (IVIS Spectrum), following i.p. injection of D-luciferin (150 mg/kg). At the end point (28 days after treatment initiation), final imaging was performed and animals were sacrificed. Thereafter, primary tumors were resected, weighed, measured and mice imaged for detection of near and distant metastases. Tumor volume was calculated by the following formula: $(A \times B^2)/2$, where $A$ is the larger and $B$ is the smaller of the two dimensions. In addition, the liver, lung and spleen were excised and imaged separately, and then fixed in Bouin's solution.

### Histological and IHC analyses

IHC analysis was performed on deparaffinized and rehydrated tissue sections from formalin-fixed, paraffin-embedded blocks of orthotopically developed pancreatic tumors as described earlier (20). All the antibodies were used at 1:100 dilutions. For histological examination, tumors and metastatic lesions were stained with hematoxylin and eosin (H&E) and visualized under microscope (×100 and ×400), and photographed.

### Protein isolation and subcellular fractionation

Total proteins from vehicle- or HNK-treated PC cells and tumor tissues were prepared in Nonidet P-40 (NP40) buffer supplemented with protease and phosphatase inhibitors. Cytoplasmic and nuclear protein fractions of PC cells were isolated using the Nuclear Extract Kit, as per manufacturer's instructions.

### Immunoblot assay

Total protein was resolved on 10% polyacrylamide gels and transferred to polyvinylidene fluoride membranes. Blots were subjected to a standard immunodetection procedure using specific antibodies against and visualized using SuperSignal West Femto Maximum sensitivity substrate kit with a LAS-3000 image analyzer.

### Collection of conditioned media

PC cells were grown in 100 mm Petri dishes up to 65–70% confluency and treated with vehicle or HNK (10 μM) for 12 h in regular media. Post-treatment, cells were washed with phosphate-buffered saline and cultured in low serum supplemented regular media for 48 h. Thereafter, conditioned media (CM) was collected, centrifuged at 300*g* for 10 min to remove cell debris and designated as CM-Veh (from vehicle-treated cells) and CM-HNK (from HNK-treated cells). To obtain CM, pancreatic stellate cells (PSCs) were grown in low serum supplemented media for 48 h, supernatant was collected, centrifuged and used in subsequent experiments.

### WST-1 assay

PSCs were seeded in 96-well plate (3000 cells/well), grown for 24 h under regular culture conditions and treated with Veh-CM or HNK-CM collected from vehicle or HNK-treated PC cells, respectively, for 72 h. In parallel, PC cells were treated with vehicle or HNK (10 μM) for 48 h, collected by trypsinization, counted and equally seeded (3000 cells/well) in 96-well plate. After overnight incubation, PC cells were treated for 72 h with CM collected form PSCs (PSCs-CM). Subsequently, viability of PSCs or PC cells was measured by WST-1 assay, and percent viability was calculated as described earlier (14,15). To examine the role of SHH, PSCs were treated with either SHH-neutralizing antibody (in case of Veh-CM) or recombinant SHH (in case of HNK-CM), and effect on cell viability was examined by WST-1 assay.

### Transfection

To understand the role of NF-κB/p65, PC cells were transiently transfected with constitutively active IKKβ mutant (pCMV-IKKβ S177E S181E) or with its control vector (pCMV) using X-tremeGENE HP DNA Transfection Reagent as per the instructions by the manufacture.

### Statistical analysis

All the experiments were performed at least three times, independently, and all data are expressed as mean ± SD. Wherever appropriate, the data were also subjected to unpaired two-tailed Student's *t*-test or analysis of variance. $P < 0.05$ was considered statistically significant.

## Results

### HNK suppresses the plating efficiency, anchorage-independent clonogenic growth and malignant phenotypes of PC cells

In our earlier study, we demonstrated the growth inhibitory potential of HNK in PC (12). Here, we extended our findings by examining the effect of HNK on the long-term growth, clonogenic potential and malignant properties of two aggressive PC cell lines (MiaPaCa and Colo-357). We first performed plating efficiency assay, which is an ideal test to monitor the long-term growth of tumor cells (21). MiaPaCa and Colo-357 cells were seeded at low density (500 cells/well), treated with HNK (0.625–5 μM) or vehicle (dimethyl sulfoxide) and incubated for 2 weeks. Our data demonstrate that the plating efficiency of MiaPaCa and Colo-357 cells was significantly and gradually decreased with the increasing concentrations of HNK. As shown in Figure 1A, we observed that MiaPaCa cells exhibited 1.7-, 3.8-, 8.21- and 51.1-folds, whereas Colo-357 exhibited 1.98-, 3.9-, 7.4- and 34.1-folds decrease in plating efficiency at 0.625, 1.25, 2.5 and 5.0 μM HNK treatment doses, respectively, as compared with the vehicle-treated controls. Further, we examined the effect of HNK on the anchorage-independent growth of PC cells by performing soft-agar-based clonogenic assay. Similar to the plating efficiency data, the clonogenic potential of HNK-treated PC cells was also reduced by 1.9-, 2.9- and 8.5-folds (in MiaPaCa) and ~1.8-, 5.2- and 17.3-folds (in Colo-357) at 0.625, 1.25 and 2.5 μM of HNK, respectively. Notably, at 5 μM of HNK treatment, no to very less visible colonies were observed in both MiaPaCa and Colo-357 cells (Figure 1B).

We next determined the effect of HNK on the aggressive malignant phenotypes of PC cells. For this, PC cells were treated with increasing doses of HNK for 48 h, and then trypsinized and used for the assessment of migration and invasion ability. We observed that the motility of PC was drastically decreased on HNK treatment. These data show that in comparison with vehicle controls, the number of migratory cells were decreased ~2.2-, 3.2-, 6.4- and 13.2-folds (in MiaPaCa) and ~1.2-, 2.8-, 7.2- and 11.3-folds (in Colo-357) at 0.625, 1.25, 2.5 and 5.0 μM of HNK, respectively (Figure 1C). Similarly, invasive potential of MiaPaCa and Colo-357 cells was also suppressed by ~1.64- to 12.9-folds and 2.4- to 11.2-folds, respectively, on HNK treatment (0.625–5 μM) as compared with vehicle-treated controls (Figure 1D). Together, these findings indicate that HNK effectively inhibits plating efficiency, clonogenic potential and malignant phenotypes of PC cells.

### HNK inhibits pancreatic tumor growth and metastasis in an orthotopic mouse model

Next, we evaluated the antitumor efficacy of HNK *in vivo* using an orthotopic xenograft mouse model of PC. For this, we chose MiaPaCa cells, which are shown to be highly tumorigenic and metastatic in mice (19). These cells were luciferase-tagged to enable non-invasive real-time monitoring of their growth. Cells were implanted directly into the mouse pancreas and tumor growth examined on alternate days by palpation. After 7 days of implantation, when tumors became palpable, mice were divided into two groups. One group of mice received a daily i.p. injection of HNK (150 mg/kg), where the other was administered only the vehicle (Figure 2A). Tumor growth was monitored once a week using IVIS imaging system following i.p. injection of D-luciferin. At the end point (28 days after treatment initiation), mice were imaged one final time and

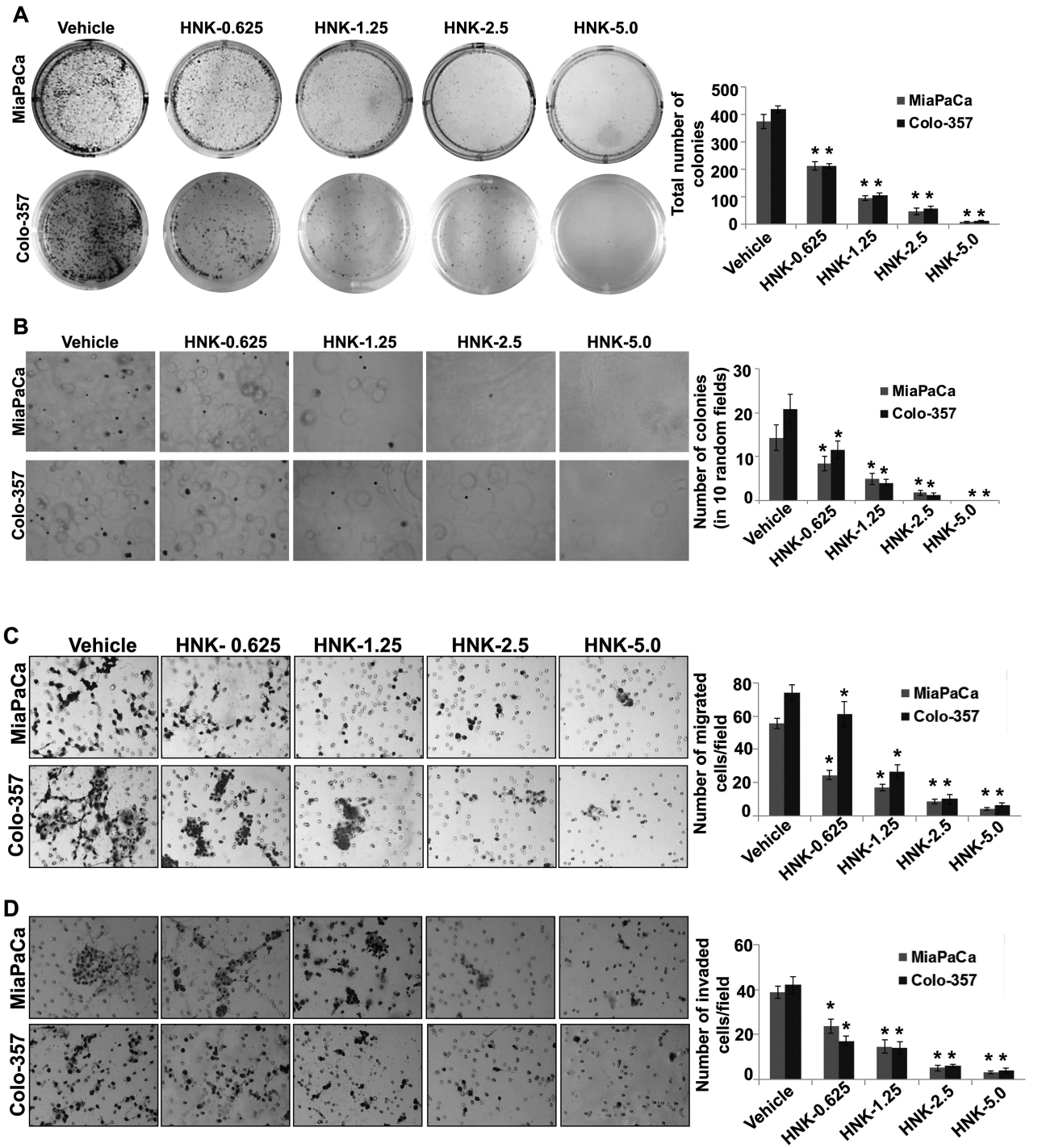


**Figure 1.** HNK inhibits growth and malignant properties of PC cells. (**A**) PC cells were seeded in six-well plates ($1 \times 10^3$ cells/well) and treated with vehicle or indicated doses of HNK. After 2 weeks of culturing, colonies were fixed, stained, photographed and quantified. (**B**) Equal volumes of agarose and growth medium were mixed and plated to form bottom layer in six-well plates. Cells were suspended in regular media mixed with an equal volume of agarose, and cell suspension-agar mix was seeded as top layer in each well. Cells were then incubated with vehicle or various concentrations of HNK (0.625–5.0 μM) under normal culture conditions, for 3 weeks for colony formation. Subsequently, colonies were stained with crystal violet, photographed and counted in 10 randomly selected fields. (**C** and **D**) PC cells were treated with various concentrations of HNK for 48 h. Thereafter, cells were then trypsinized, counted, suspended in serum-free media and seeded equally (C) for motility [$5 \times 10^5$ (MiaPaCa) and $1 \times 10^6$ (Colo-357) cells/well] assay on non-coated membranes and (D) for invasion on Matrigel-coated polycarbonate membrane [$2.5 \times 10^5$ (MiaPaCa) and $5 \times 10^5$ (Colo-357) cells/well]. Media supplemented with 10% fetal bovine serum was used as chemoattractant in lower chamber. Cells were allowed to migrate/invade for 16 h, and then, cells remaining in the upper portion were removed. Cells that had migrated/invaded were fixed, stained with Diff-Quick cell staining kit (Dade Behring), mounted on slides and counted in 10 random fields under microscope. Bars represent the mean ± SD ($n = 3$). *$P < 0.05$.

then sacrificed. Non-invasive imaging analysis showed that tumor growth in HNK-treated group of mice was significantly decreased in comparison with the vehicle-treated mice group (Figure 2B and C). Moreover, our end-point measurements revealed smaller tumors with average weight of 0.77 g and size of 99.6 $mm^3$ in HNK-treated mice, as compared with average

weight of 2.88 g and size of 1361.0 mm$^3$ in vehicle-treated mice (Figure 2D and E).

After removal of primary tumors, mice were imaged again to examine the presence of metastatic lesions and secondary metastatic organs collected. Metastatic dissemination of pancreatic tumor cells to various distinct organs [liver (66.6%), lungs (66.6%) and spleen (83.3%)] of mice was observed in majority of the mice of vehicle-treated group, as was evident from the strong luminescent signal. No metastases were detected in any of the mice, which received HNK (Figure 3A–C). The presence or absence of metastatic tumor-cell nests to secondary sites was further confirmed by microscopic analysis of H&E-stained tissue sections (Figure 3D). Altogether, our data suggest that HNK suppresses pancreatic tumor growth and eliminates metastatic spread.

## Desmoplasia is decreased in pancreatic tumor xenografts of HNK-treated mice

Extensive desmoplasia is a fundamental characteristic of pancreatic tumors, which has been suggested to be of significance from the pathobiological and clinical standpoints (22–24). Therefore, we next examined the effect of HNK on the desmoplastic reaction in orthotopic pancreatic tumors. To accomplish this, tumor tissue sections were stained with H&E and examined under microscope. The presence of excessive dense fibrotic area was revealed in the tumors of control group mice, whereas it was only minimal in sections of tumor tissues from HNK-treated group of mice (Figure 4A). The presence of desmoplasia was further confirmed by immunostaining for specific markers of desmoplasia, viz. α-SMA and collagen I (13). These data demonstrated intense staining of α-SMA (Figure 4B) and collagen I (Figure 4C) in tumor tissue sections from vehicle-treated group, whereas weak or no staining was detected in tumor sections of HNK-treated mice (Figure 4B and C). Taken together, these findings suggest that HNK inhibits desmoplastic reaction in pancreatic tumors.

## HNK interferes with tumor–stromal cross-talk by downregulating the expression of CXCR4 and SHH in PC cells

Previous studies from our lab and elsewhere have provided strong support for the role of CXCR4 and SHH in pancreatic tumor growth, metastasis and desmoplasia by enabling bidirectional tumor–stromal cross-talk (15,17,18,25–27). Therefore, we examined the expression status of CXCR4 and SHH in tumor sections by IHC analyses. Data show a decrease in CXCR4 and SHH expression in pancreatic tumors of HNK-treated group, as compared with that of vehicle-treated group (Figure 5A). This is further supported by the immunoblotting data from proteins isolated from fresh-frozen tumor xenografts (Figure 5B). To further confirm these observations, we treated both MiaPaCa and Colo-357 cells in culture with various doses of HNK or vehicle and examined the expression of CXCR4 and SHH by quantitative reverse transcription–PCR and immunoblot assays. Treatment with HNK for 48 h resulted in a dose-dependent decrease in the expression of both CXCR4 and SHH at mRNA (Supplementary Figure 1 is available at *Carcinogenesis* Online) and protein

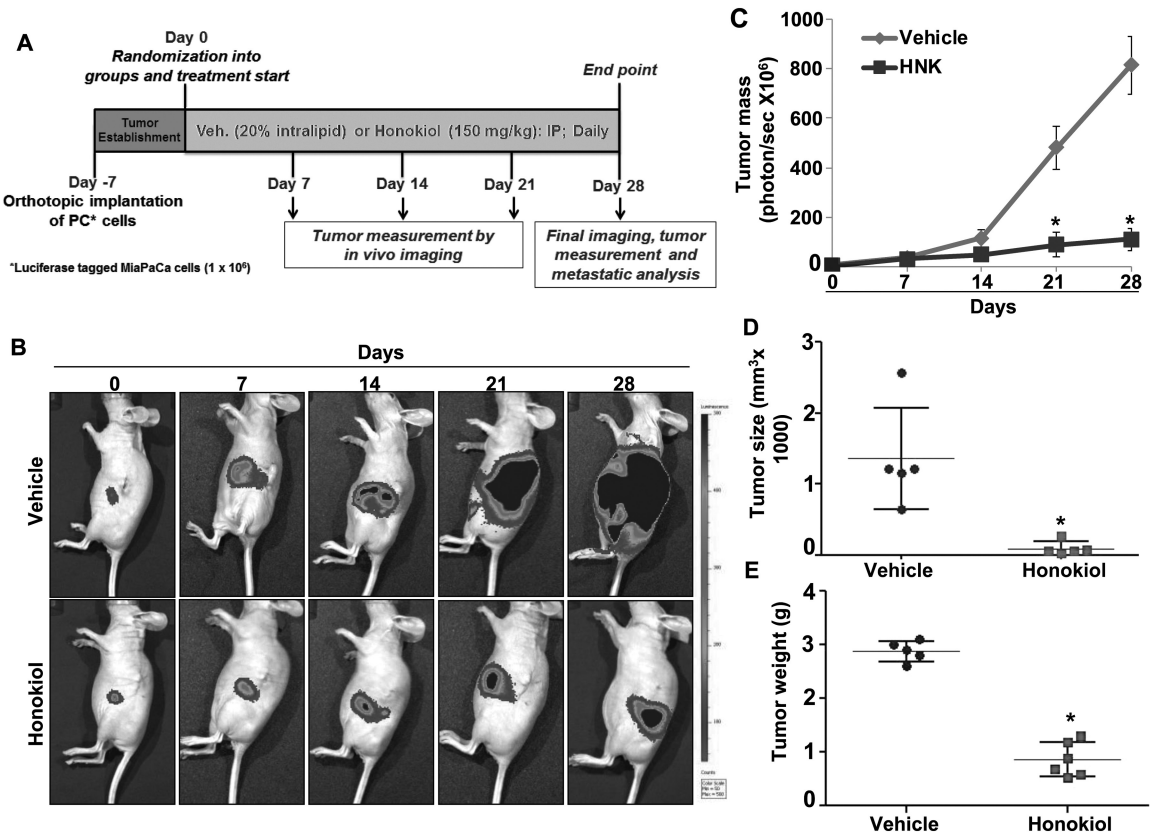


**Figure 2.** HNK decreases tumorigenicity of PC cells in orthotopic mice model. (**A**) Schematic representation of *in vivo* treatment strategy. (**B**) Tumor growth was monitored by measuring luminescence in vehicle- and HNK-treated mice ($n$ = 6 per group) once a week using IVIS imaging station following i.p. injection of D-luciferin. Images are representative of mice from both the groups at different time points. (**C**) Tumor growth curve (total photons per second) showing tumor growth at different time points in vehicle- and HNK-treated group. (**D**) Volume and (**E**) weight of the tumors from vehicle- and HNK-treated group at the end point.

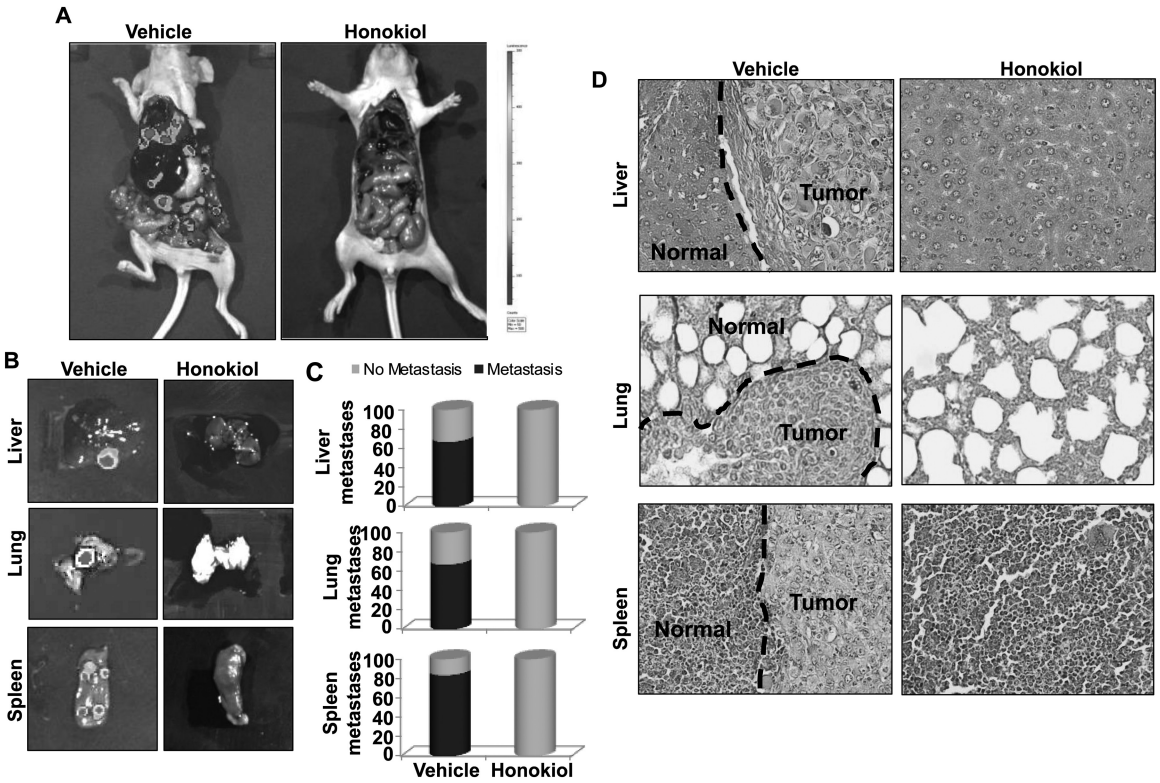


**Figure 3.** HNK inhibits metastasis of PC cells. (**A**) Following tumor excision, mice from each group ($n$ = 6 per group) were imaged to visualize metastases to secondary organs. Images are representative of all the mice from both the treatment groups. (**B**) Livers, lungs and spleens were carefully removed from the mice and imaged for metastatic lesions. (**C**) Graphical representation showing incidence of metastasis to different secondary organs. Black and gray colors represent positive and negative incidence. (**D**) Metastatic tissues (liver, lung and spleen) were fixed in Bouin's solution, paraffin-embedded and cut into 5 µ sections. Subsequently, H&E staining was performed and sections analyzed microscopically to detect the presence or absence of tumor cell nests. Magnifications = ×200.

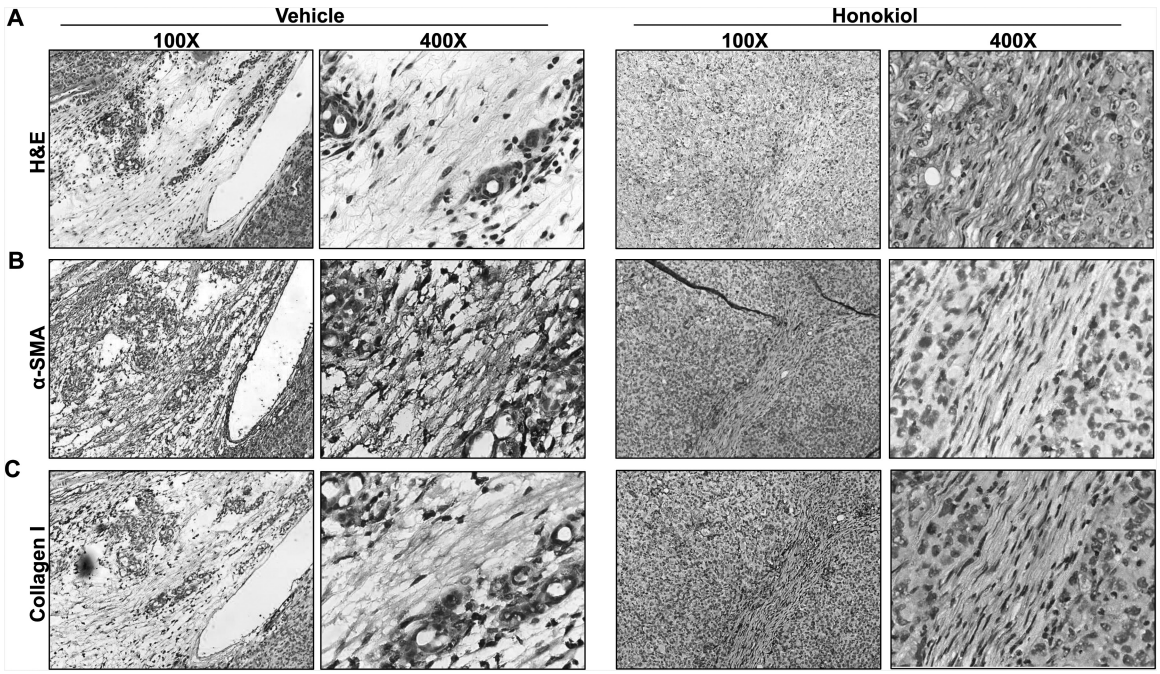


**Figure 4.** HNK suppresses pancreatic tumor-associated desmoplastic region. (**A**) Tissue sections from formalin-fixed tumors derived from vehicle- and HNK-treated group of mice were subjected to H&E staining to study histopathological characteristics. (**B** and **C**) IHC analysis was performed on tumor sections to detect the expression of extracellular matrix proteins, (B) myofibroblast maker, α-SMA and (C) collagen I.

levels (Figure 5C). To confirm the role of SHH downregulation in decreased tumor–stromal cross-talk, we treated PSCs with CM from either vehicle (Veh-CM) or HNK-treated PC cells (HNK-CM). Significant growth induction ($P < 0.01$) was observed only in PSCs treated with Veh-CM (Figure 5C). Furthermore, this growth induction was abrogated when Veh-CM was preincubated

with anti-SHH antibodies, whereas it was induced in HNK-CM-treated PSCs on addition of exogenous recombinant SHH (Figure 5D). In a reverse approach, when we exposed vehicle or HNK-pretreated PC cells with CM of PSCs (CM-PSCs), we observed significantly less growth induction in case of HNK-pretreated MiaPaCa and Colo-357 (44.1 and 51.5%, respectively) cells as compared with that pretreated with vehicle (Figure 5E). Further, vehicle- and HNK-treated PC cells were incubated with AMD3100, a CXCR4 antagonist, 30 min. prior to their exposure to CM-PSCs to ascertain the role of CXCR4 in the CM-PSCs-mediated growth induction. Data demonstrate that CM-PSCs-induced growth of PC cells is remarkably abrogated when they are pretreated with AMD3100, whereas no effect of AMD3100 is observed in HNK-pretreated PC cells, suggesting that CXCR4 downregulation is involved in the poor response of HNK-treated PC cells to CM-PSCs (Figure 5E). Together, these findings establish the role of HNK in interfering with tumor–stromal cross-talk via CXCR4 and SHH downregulation.

### HNK-induced inhibition of NF-κB is responsible, in part, for downregulation of CXCR4 and SHH

We previously reported HNK as a potent inhibitor of NF-κB activation in PC cells (12). Since NF-κB is also a transcriptional regulator for both CXCR4 and SHH (15,18), we examined its role in their observed downregulation in HNK-treated PC cells. For this, PC cells were transfected with plasmids either expressing constitutively active mutant of IKKβ (IKKβ-SSEE) or a control vector (pCMV) prior to the HNK treatment. The effects of these transfections on the transcriptional activity and nuclear localization of NF-κB were examined following HNK treatment. Transcriptional activity (Figure 6A) and nuclear localization of NF-κB (Figure 6B) was inhibited in control vector-transfected cells on HNK treatment; where no inhibitory effects were observed in MiaPaCa and Colo-357 cells transfected with IKKβ mutant (Figure 6A and B). Moreover, when we examined the effect of restored NF-κB activation on the HNK-mediated downregulation of CXCR4 and SHH, we observed that the expression of CXCR4 and SHH was regained to an appreciable extent, but not completely (Figure 6C). These findings suggest that suppression of NF-κB activation by HNK is, at least partly, responsible for its inhibition of CXCR4 and SHH expression in PC cells.

## Discussion

PC is a difficult cancer to manage and treat. The outcomes of patients with this deadly cancer have not improved much over last several decades, with most chemotherapies affording only minor improvements in overall survival (1). In an earlier study, we observed an anticancer activity of HNK in PC cells through induction of cell-cycle arrest and apoptosis (12). Moreover, our findings established, for the first time, NF-κB as a molecular target for HNK, which was also suggested to mediate HNK-potentiated chemosensitization. Since then, HNK has been shown to affect NF-κB signaling in lung (28) and colon (10)

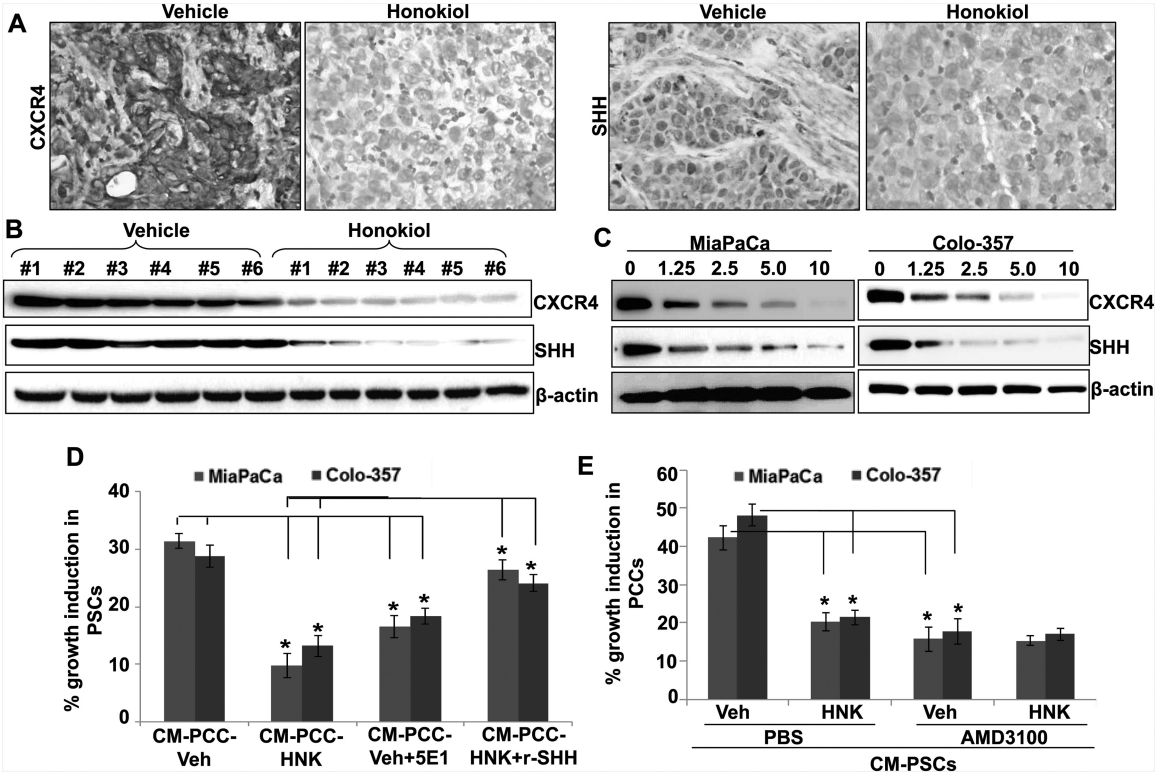


**Figure 5.** HNK inhibits tumor–stromal interaction by suppression of CXCR4 and SHH expression in PC cells. (**A**) IHC analysis of paraffin-embedded pancreatic tumor specimens was performed to examine CXCR4 and SHH expression. (**B**) Total protein from orthotopically developed pancreatic tumors was collected and subjected to immunoblot analysis to examine the expression of CXCR4 and SHH. (**C**) PC cells were treated with vehicle or HNK (1.25–10 μM) for 72 h. Thereafter, total protein was extracted and CXCR4 and SHH expression was analyzed by immunoblot assay. β-Actin was used as loading control. (**D**) PSCs were grown in 96-well plate and treated with Veh-CM and HNK-CM in the presence or absence of SHH-neutralizing antibody (5E1) and recombinant SHH (r-SHH), respectively, for 72 h, and effect on growth was determined by WST-1 assay. (**E**) PC cells pretreated with vehicle or HNK (10 μM; 48 h) were equally seeded (3000 cells/well) in 96-well plate. After overnight culturing, cells were treated with phosphate-buffered saline or AMD3100 (CXCR4 antagonist; 5 μg/ml) 30 min prior to their exposure of CM collected form PSCs (CM-PSCs) for 72 h, and effect on growth was determined by WST-1 assay. Data (mean ± SD; $n = 3$) shown as change in growth in comparison with control.*$P \leq 0.05$.

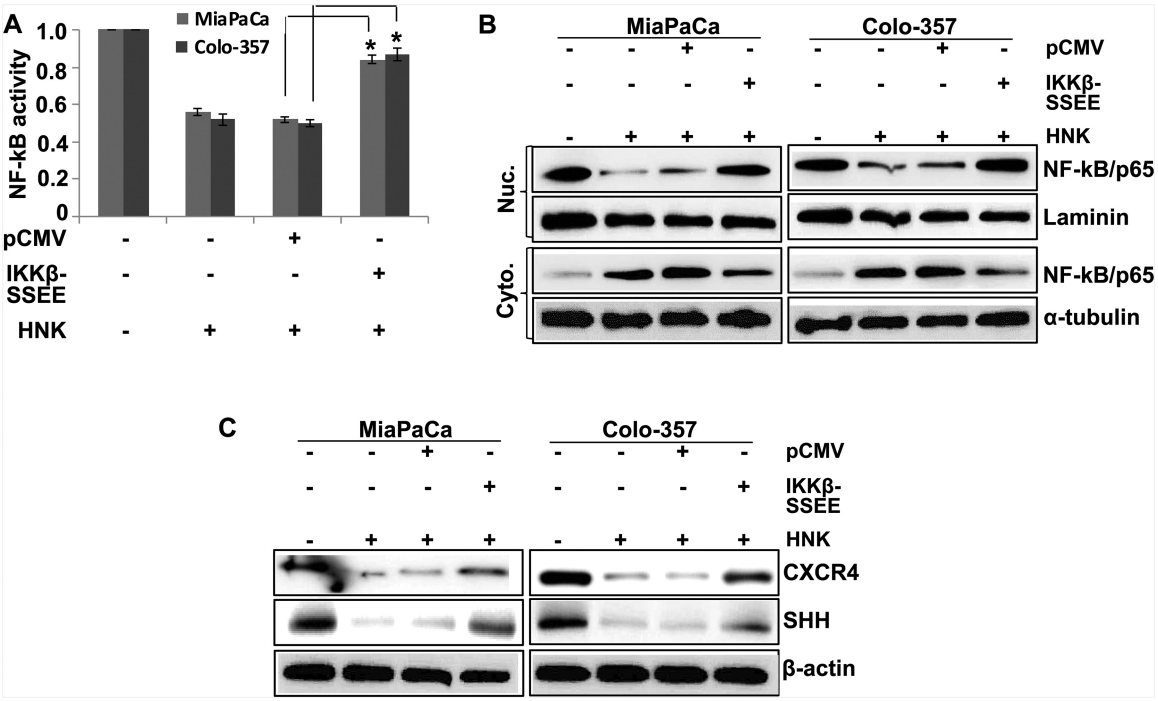


**Figure 6.** HNK-downregulated expression of CXCR4 and SHH is partially mediated by NF-κB. PC cells were transfected with constitutively active IKKβ mutant (IKKβ-SSEE) or empty vector (pCMV). (**A**) After 48-h transfection, cells were again transfected with NF-κB-luciferase promoter-reporter constructs for 24 h, treated with HNK, and NF-κB transcriptional activity was examined 48 h of HNK treatment. Bars represent the mean of triplicates ± SEM, *$P < 0.05$. (**B**) Nuclear and cytoplasmic fractions were prepared after 24 h of HNK treatment, and expression level of NF-κB was examined by immunoblot assay. (**C**) Cells were treated with HNK for 48 h; total protein was isolated; and expression of CXCR4 and SHH was examined by immunoblot assay. Laminin (for nuclear fraction), α-tubulin (for cytoplasmic fraction) and β-actin (for total protein) were used as loading controls.

cancer cells as well. The present study further affirms the significance of NF-κB targeting by HNK that leads to downregulation of molecules involved in tumor–stromal cross-talk and thus suggest wider implications for antitumor efficacy of HNK.

Pancreatic tumors are highly aggressive in nature and, in most cases, have already metastasized at the time of its diagnosis (29). Metastasis is the major cause of cancer-related deaths, and this is true for PC as well (30). In fact, most pancreatic tumors, if not metastasized, are so genetically advanced that their resection is feared to cause metastases (31). Clearly, we need approaches that could target the aggressive nature of pancreatic tumors. In this regard, our data demonstrating the suppressive effect of HNK not only on tumor growth but also on malignant phenotypes are highly significant and could have implications for both PC therapy and prevention. Another unique characteristic of PC is existence of high desmoplasia, which is suggested to promote lymphangiogenesis, metastasis and chemoresistance (22,24). It is also being explored as a factor that influences the balance between immune-dependent and immune-independent regulation of tumor growth (23). In our study, we observed an inhibitory effect of HNK on desmoplasia, as characterized by reduced secretion of extracellular matrix protein (collagen I) and diminished staining for myofibroblast marker (a-SMA). Myofibroblasts are a major component of desmoplastic pancreas and originate from activated PSCs (32). Thus, our data provided direct evidence for a dual impact of HNK on pancreatic tumors through targeting its tumor and stromal compartments.

CXCR4 is a chemokine receptor for CXCR12 (also called stromal-derive factor 1). CXCR12/CXCR4 signaling is shown to play important roles in tumor–stromal cross-talks in several tumors, wherein CXCR12 secreted by stromal cells in the tumor microenvironment stimulates the growth of CXCR4-expressing tumor cells (16). In the current study, we noted an inhibitory effect of HNK on this signaling and associated functional consequences. Not only did we observe downregulation of CXCR4 by HNK, we also found significant disruption of tumor–stromal interactions. CM from HNK-treated tumor cells failed to stimulate growth of PSCs and vice versa. Inhibition of CXCR4 and the tumor–stromal cross-talk by HNK can have big implications because of the documented role of CXCR4/CXCR12 signaling in cancer metastasis (33) and drug resistance (14,34). Activation of this signaling axis induces diverse signaling pathways that act independently and cross-talk with each other and/or other active signaling pathways to promote a variety of cancer-relevant cellular and molecular responses (16,35). Besides, we also observed an inhibition of SHH expression by HNK, which is highly relevant to tumor–stromal interactions (13,15,25). Tumor–stromal cross-talk was significantly affected when SHH was downregulated, either as a consequence of HNK treatment or its functional inhibition by the use of SHH antibody as a proof of principal. Abrogation of HNK activity by recombinant SHH further supported the mechanistic importance of SHH in the disruption of tumor–stromal interactions by HNK. It thus appears that HNK impacts both tumor and stromal compartments by inhibiting the cross-talk between tumor and stroma cells through its modulation of CXCR4/CXCR12 axis and downregulation of SHH.

The role of NF-κB, an oncogenic transcription factor, in promoting several biological processes of cancer significance, such as proliferation, survival, invasion and metastasis, and therapy resistance has been very well documented (36). Emerging evidence confirms the constitutive activation of NF-κB in tumors of several types including PC (37,38), wherein its aberrant activation enhances the transcription of proinflammatory and protumorigenic genes. Similar to our earlier findings (12),

we found that HNK inhibited NF-κB in pancreatic tumor cells. In addition, our mechanistic studies revealed the partial involvement of NF-κB in HNK-mediated downregulation of CXCR4 and SHH in PC cells. We have earlier established the role of NF-κB in direct transcriptional regulation of CXCR4 and SHH in PC cells (15,18). Since NF-κB acts as a downstream and upstream effector of CXCL12/CXCR4 signaling in a positive feedback mechanism, it not only sustains the increasing activation of this signaling loop (15,39) but also amplifies the impact on tumor phenotypes through activation of several other CXCR4-downstream signaling pathways. More importantly, through regulation of SHH, it can further diversify impact by involving stromal cells and initiating a bidirectional tumor–stromal cross-talk (15). Therefore, the concurrent activation of several cancer-relevant pathways promotes the proliferation, survival and metastasis of tumor cells (20,40,41). In accordance with this, we observed that HNK treatment inhibited the growth and metastasis of pancreatic tumor cells in orthotopic mouse model. These findings are of high clinical importance from the standpoints of developing novel HNK-based therapeutic and prevention strategies. Moreover, these findings establish the mechanistic bases for the inhibitory effects of HNK against PC.

Taken together, our study is indicative of a multifaceted antitumor efficacy of HNK against PC cells, both *in vitro* and *in vivo*. Our results support the role of HNK in suppressing metastatic machinery through inhibition of NF-κB and its downstream targets CXCR4 and SHH, resulting not only in suppression of tumor growth but also in a complete remission of metastasis in an orthotopic mouse model. This is also accompanied by an inhibitory effect of HNK on desmoplasia through inhibition of tumor–stromal interactions and could be of significance from therapeutic standpoints. Thus, our results hold a lot of promise for the eventual goal of developing HNK as an effective therapeutic or preventive agent through its targeting of signaling pathways of high significance in PC.

## Supplementary material

Supplementary Figure 1 can be found at http://carcin.oxfordjournals.org/

## Funding

NIH/NCI (CA167137 and CA175772 to A.P.S.); USAMCI.
*Conflict of Interest Statement*: None declared.

## References

1. Garrido-Laguna, I. et al. (2015) Pancreatic cancer: from state-of-the-art treatments to promising novel therapies. Nat. Rev. Clin. Oncol., 12, 319–334.
2. Siegel, R.L. et al. (2016) Cancer statistics, 2016. CA Cancer J. Clin., 66, 7–30.
3. Moore, M.J. et al.; National Cancer Institute of Canada Clinical Trials Group. (2007) Erlotinib plus gemcitabine compared with gemcitabine alone in patients with advanced pancreatic cancer: a phase III trial of the National Cancer Institute of Canada Clinical Trials Group. J. Clin. Oncol., 25, 1960–1966.
4. Von Hoff, D.D. et al. (2013) Increased survival in pancreatic cancer with nab-paclitaxel plus gemcitabine. N. Engl. J. Med., 369, 1691–1703.
5. Allison, M. (2012) Hedgehog hopes lifted by approval and stung by failure. Nat. Biotechnol., 30, 203.
6. Newman, D.J. (2008) Natural products as leads to potential drugs: an old process or the new hope for drug discovery? J. Med. Chem., 51, 2589–2599.
7. Kneller, R. (2010) The importance of new companies for drug discovery: origins of a decade of new drugs. Nat. Rev. Drug Discov., 9, 867–882.
8. Dias, D.A. et al. (2012) A historical overview of natural products in drug discovery. Metabolites, 2, 303–336.
9. Arora, S. et al. (2012) Honokiol: a novel natural agent for cancer prevention and therapy. Curr. Mol. Med., 12, 1244–1252.
10. Hua, H. et al. (2013) Honokiol augments the anti-cancer effects of oxaliplatin in colon cancer cells. Acta Biochim. Biophys. Sin. (Shanghai), 45, 773–779.
11. Leeman-Neill, R.J. et al. (2010) Honokiol inhibits epidermal growth factor receptor signaling and enhances the antitumor effects of epidermal growth factor receptor inhibitors. Clin. Cancer Res., 16, 2571–2579.
12. Arora, S. et al. (2011) Honokiol arrests cell cycle, induces apoptosis, and potentiates the cytotoxic effect of gemcitabine in human pancreatic cancer cells. PLoS One, 6, e21573.
13. Bailey, J.M. et al. (2008) Sonic hedgehog promotes desmoplasia in pancreatic cancer. Clin. Cancer Res., 14, 5995–6004.
14. Bhardwaj, A. et al. (2014) CXCL12/CXCR4 signaling counteracts docetaxel-induced microtubule stabilization via p21-activated kinase 4-dependent activation of LIM domain kinase 1. Oncotarget, 5, 11490–11500.
15. Singh, A.P. et al. (2012) CXCL12/CXCR4 protein signaling axis induces sonic hedgehog expression in pancreatic cancer cells via extracellular regulated kinase- and Akt kinase-mediated activation of nuclear factor κB: implications for bidirectional tumor-stromal interactions. J. Biol. Chem., 287, 39115–39124.
16. Sun, X. et al. (2010) CXCL12/CXCR4/CXCR7 chemokine axis and cancer progression. Cancer Metastasis Rev., 29, 709–722.
17. Xu, X. et al. (2014) Sonic hedgehog-Gli1 signaling pathway regulates the epithelial mesenchymal transition (EMT) by mediating a new target gene, S100A4, in pancreatic cancer cells. PLoS One, 9, e96441.
18. Arora, S. et al. (2013) An undesired effect of chemotherapy: gemcitabine promotes pancreatic cancer cell invasiveness through reactive oxygen species-dependent, nuclear factor kappaB- and hypoxia-inducible factor 1alpha-mediated up-regulation of CXCR4. J. Biol. Chem., 288; 21197–21207.
19. Srivastava, S.K. et al. (2015) MYB is a novel regulator of pancreatic tumour growth and metastasis. Br. J. Cancer, 113, 1694–1703.
20. Bhardwaj, A. et al. (2014) Restoration of PPP2CA expression reverses epithelial-to-mesenchymal transition and suppresses prostate tumour growth and metastasis in an orthotopic mouse model. Br. J. Cancer, 110, 2000–2010.
21. Munshi, A. et al. (2005) Clonogenic cell survival assay. Methods Mol. Med., 110, 21–28.
22. Erkan, M. et al. (2012) The role of stroma in pancreatic cancer: diagnostic and therapeutic implications. Nat. Rev. Gastroenterol. Hepatol., 9, 454–467.
23. Puré, E. et al. (2016) Can targeting stroma pave the way to enhanced antitumor immunity and immunotherapy of solid tumors? Cancer Immunol. Res., 4, 269–278.
24. Olive, K.P. et al. (2009) Inhibition of Hedgehog signaling enhances delivery of chemotherapy in a mouse model of pancreatic cancer. Science, 324, 1457–1461.
25. Bailey, J.M. et al. (2009) Sonic hedgehog paracrine signaling regulates metastasis and lymphangiogenesis in pancreatic cancer. Oncogene, 28, 3513–3525.
26. Li, X. et al. (2014) Sonic hedgehog paracrine signaling activates stromal cells to promote perineural invasion in pancreatic cancer. Clin. Cancer Res., 20, 4326–4338.
27. Marchesi, F. et al. (2004) Increased survival, proliferation, and migration in metastatic human pancreatic tumor cells expressing functional CXCR4. Cancer Res., 64, 8420–8427.
28. Singh, T. et al. (2013) Honokiol inhibits non-small cell lung cancer cell migration by targeting PGE(2)-mediated activation of beta-catenin signaling. PLoS One, 8, e60749.
29. Vincent, A. et al. (2011) Pancreatic cancer. Lancet, 378, 607–620.
30. Das, S. et al. (2015) Pancreatic cancer metastasis: are we being pre-EMTed? Curr. Pharm. Des., 21, 1249–1255.
31. Paik, K.Y. et al. (2012) Analysis of liver metastasis after resection for pancreatic ductal adenocarcinoma. World J. Gastrointest. Oncol., 4, 109–114.
32. Omary, M.B. et al. (2007) The pancreatic stellate cell: a star on the rise in pancreatic diseases. J. Clin. Invest., 117, 50–59.
33. Guo, F. et al. (2016) CXCL12/CXCR4: a symbiotic bridge linking cancer cells and their stromal neighbors in oncogenic communication networks. Oncogene, 35, 816–826.

34. Duda, D.G. et al. (2011) CXCL12 (SDF1alpha)-CXCR4/CXCR7 pathway inhibition: an emerging sensitizer for anticancer therapies? Clin. Cancer Res., 17, 2074–2080.
35. Liu, X. et al. (2014) Activation of STAT3 is involved in malignancy mediated by CXCL12-CXCR4 signaling in human breast cancer. Oncol. Rep., 32, 2760–2768.
36. Baud, V. et al. (2009) Is NF-kappaB a good target for cancer therapy? Hopes and pitfalls. Nat. Rev. Drug Discov., 8, 33–40.
37. Lessard, L. et al. (2006) Nuclear localization of nuclear factor-kappaB p65 in primary prostate tumors is highly predictive of pelvic lymph node metastases. Clin. Cancer Res., 12, 5741–5745.
38. Wharry, C.E. et al. (2009) Constitutive non-canonical NFkappaB signaling in pancreatic cancer cells. Cancer Biol. Ther., 8, 1567–1576.
39. Helbig, G. et al. (2003) NF-kappaB promotes breast cancer cell migration and metastasis by inducing the expression of the chemokine receptor CXCR4. J. Biol. Chem., 278, 21631–21638.
40. Fan, Y. et al. (2013) NF-kappaB and STAT3 signaling pathways collaboratively link inflammation to cancer. Protein Cell, 4, 176–185.
41. Wen, W. et al. (2015) Synergistic anti-tumor effect of combined inhibition of EGFR and JAK/STAT3 pathways in human ovarian cancer. Mol. Cancer, 14, 100.